MODELING OF REAL UT TRANSDUCER FIELD/FLAW INTERACTIONS

B. A. Barna

EG&G Idaho, Inc.
Idaho Falls, ID 83415

INTRODUCTION

When a component is inspected using ultrasonics, a number of variables are specified to optimize detection and characterization of flaws. It would be quite useful to have a model of the field/flaw interaction that would allow selection of the best transducer and inspection geometry for a given set of potential flaws. Moreover, if the model can give insight into the physics of the field/flaw interaction, it can be used to select features in the signals received that best characterize the flaw.

The detectable signal that results from the interaction between a transducer field and a flaw reflecting it is a composite of the effects of many physical phenomena. Some of the major features of this interaction are shown schematically in Fig. 1. If one could quantitatively account for each of these features and the process is linear, it is conceivable that the output signal from such a system could be accurately predicted. In practice, however, the problem is so complex that currently no such model exists for a complete solution of the problem.

Partial solutions, however, can be obtained using simplifying assumptions. One of the most popular of these is that a plane ultrasonic wave

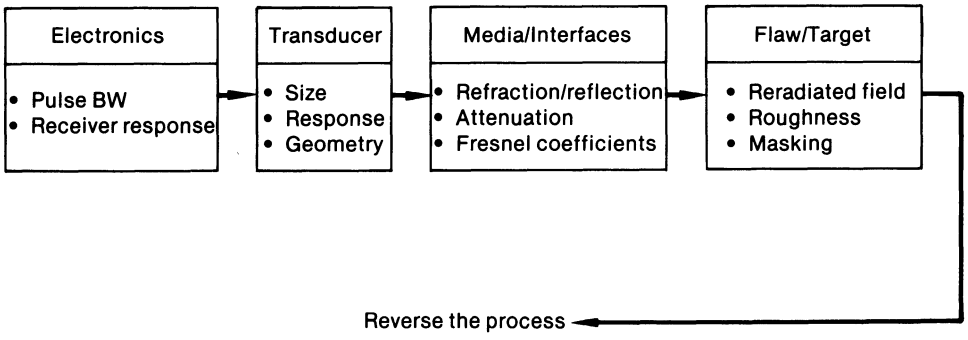

Fig. 1. Elements of the tranducer field and flaw interaction.

is incident on a flaw whose dimensions are on the order of the acoustic wavelength. In many cases this allows a fairly rigorous calculation of the scattered wave from the flaw, but it ignores the spatial features of the incident wave from a real transducer which can deviate significantly from a plane wave. Also, many flaws of critical interest are not adequately modeled by such approximations either because they are much larger than typical UT wavelengths or because they possess unique reflecting features (e.g., surface-breaking fatigue cracks that mimic a corner reflector).

In contrast to the plane wave approximation, this study models the field/flaw interaction with an integration of the portion of the transducer field that is reflected by the flaw. Essentially, this is a short wavelength approximation in which the scattering due to the flaw is treated as a specular reflection back to the transducer. In principle, however, there is no reason the scattering from the flaw cannot be included in the model, and future versions will include this feature.

The system investigated was a vertical surface-breaking crack being insonified with a refracted shear wave in an immersion tank as depicted in Fig. 2. With this geometry, one of the most unique features of the model was an allowance for the shape of the acoustic pulse wavefronts as they impinged upon the refracting surface of the crack sample.

It should be noted that a number of approximations are made in this model so that a calculational structure can be developed that will allow the physics of the field/flaw interaction to be more easily visualized and understood. The model can be interactively run on small computers at little cost so that a user can modify parameters easily and determine their effect on the predicted signal from a flaw. In this sense, this work complements the more precise and calculationally intense field codes that provide more detailed results but little physical understanding. A description of the details of the model and a comparison of its predictions with experimental measurements follows.

DESCRIPTION OF THE MODEL

The model operates in the Fourier domain and assumes that a discrete Fourier transform is the "input" spectrum for the given transducer. This spectrum is then modified at each frequency by calculating what angular portion of the field is reflected by the flaw and what the reflection and transmission coefficients are for the angle of incidence on the surface of refraction. The calculation is performed at each discrete frequency because the directivity or pressure distribution of the sound field as well as the shape of the wavefront vary as a function of frequency.

The angular portion of the field reflected by the crack is calculated by deriving a projection of the crack on the refracting surface. To derive this projection, it is necessary to make some assumptions about the nature of the transducer field. If the frequency component being analyzed is sufficiently high that the refracting surface is greater than 2 to 3 nearfield lengths away from the transducer, the transducer can be approximated by a point source of sound with spherically diverging wavefronts. This allows one to iteratively calculate two extreme rays from the point source, one of which intersects the crack tip while the other bounces from the back wall to the crack tip.

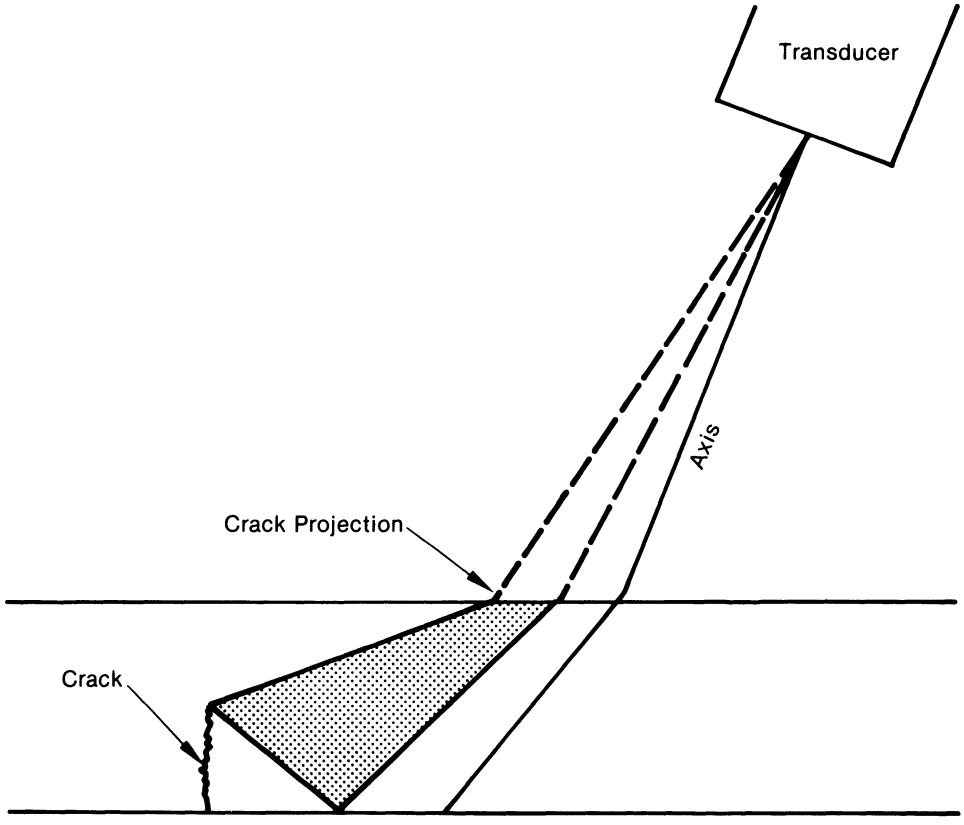

Fig. 2. Geometry of the setup used in model calculations and experiments.

While this provides a good approximation for the farfield, it is not as accurate when the frequency being analyzed is lower and the refracting surface is located at or within the nearfield. In this case the wavefront shape is no longer spherical and, in fact, has quite complex behavior. Fig. 3 shows the wavefront shape at four different frequencies for a 12.7 mm transducer approximately 65 mm away from the face. At the higher frequencies when the axial position approaches the nearfield length, the wavefront flattens near the center of the beam where the sound pressure is highest. This implies that at these higher frequencies it would be more accurate to calculate the projection of the crack on the refracting surface using an assumption of a plane wavefront.

A simple but effective way to incorporate the changing wavefront shape in the model is to calculate a projection of the crack onto the refracting surface using first the point source ray trace and then a plane wave ray trace. Each projection defines two angular extremes with respect to the axis of the transducer. These extremes are then combined as a weighted average with the weighting factor being an exponential function of the frequency component being analyzed. If the frequency is high, the angular extremes are those which would be expected from a plane wave projection of the crack; if it is low, they are what would be derived using a spherical wave.

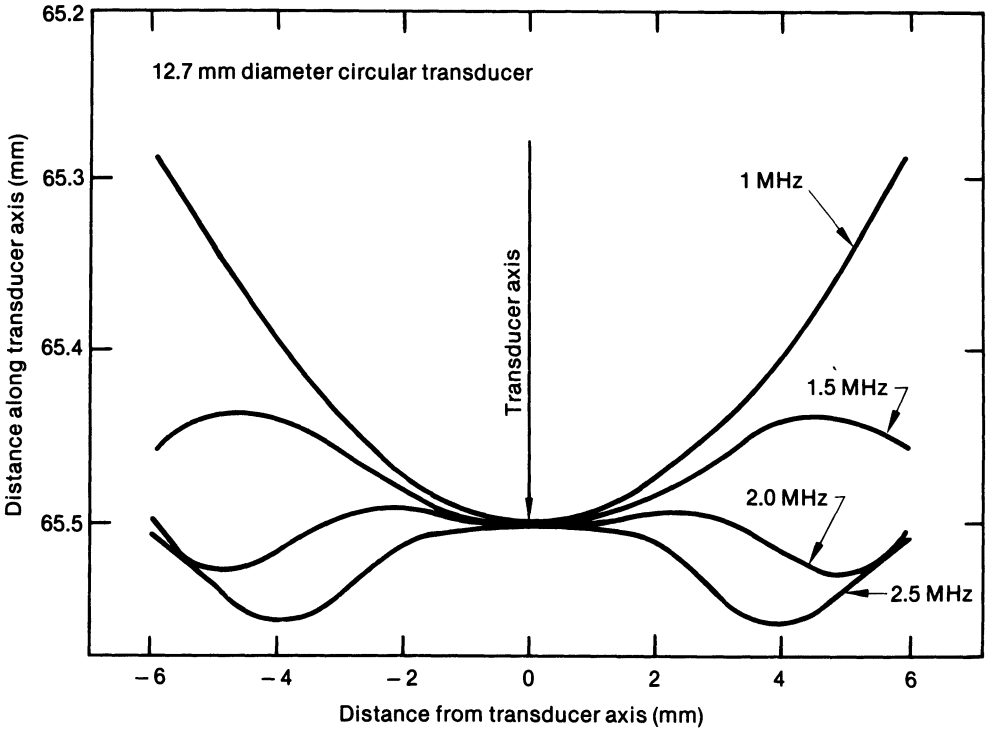

Fig. 3. Approximate wavefront shapes at four different frequency components.

Once these two angular extremes are defined, the sound pressure over the crack projection at the refracting surface can be approximated by integrating a function representing the sound pressure as a function of angle from the center of the transducer. A good, albeit not perfect, functional representation of this pressure distribution is

$$\frac{2J_1(ka \sin \theta)}{(ka \sin \theta)}$$

where

k = the wavenumber
a = the transducer radius
θ = the angle measured from the axis of the transducer.

This Bessel function representation is strictly only applicable beyond several nearfield lengths, but for this first approximation of the model it is an efficient and relatively accurate approximation.

The actual integration is accomplished by expanding

$$\frac{2J_1(x)}{x}$$

as a power series, integrating term by term, and iterating until enough terms have been included for convergence. The result of the integration is used as a multiplier of the amplitude value of the input spectra at the frequency component being analyzed.

The only other modification to the input spectrum that is currently part of the model is a term that represents the effects of the transmission coefficients at the refracting interface. To define this term, an angle of incidence is calculated. This is again a weighted average of the high and low frequency ray traces to the root of the crack. This incident angle is then used in the solution of the Fresnel equations to obtain transmission coefficients which are used to multiply the amplitude value of the input spectra at the frequency value being analyzed.

In summary then, one must supply an input spectrum, the transducer size, crack size, physical constants of the media, and geometric factors such as locations and incident angle. From this information, the model calculates an "output" spectrum by

1) Calculating a projection of the flaw onto the refracting surface for
    a) high frequency limit (plane wave source)
    b) low frequency limit (point source)
2) Blending the projections based on the current frequency component being analyzed
3) Integrating the sound pressure function over the projection
4) Calculating the transmission coefficients (water/steel-steel/water)
5) Modifying the component of the input spectrum.

COMPARISON OF PREDICTIONS WITH EXPERIMENT

A number of comparisons were made between the output spectra of the model and experimental data. The parameters which were varied were crack and electric discharge machined (EDM) notch size (0.75 to 6.0 mm), transducer frequency (2.25 and 5.0 MHz), transducer diameter (12.7 and 6.4 mm), and water path (30 to 130 mm). Due to lack of space, only a few of the comparisons will be shown here. In all cases the incident angle was 20° in a water bath and the flaws were in stainless steel bars 15 mm thick. Both fatigue cracks and EDM notches were used, but only the notch data are shown since the fatigue crack results were quite similar and the notch dimensions are more precisely known. The experimental or measured spectra were obtained from the time waveform after gating out any tip diffracted signal. Only the "root" signal was used in the analysis.

Fig. 4(a) shows the predicted spectra of the model when the transducer is moved parallel to the bar surface off the peak flaw signal in 2.5 mm increments. The transducer used was a 6.35 mm diameter 5 MHz at a water path of 130 mm. A shift to lower peak frequencies is predicted, and this is readily understood as the result of off-axis sampling of the sound field by the flaw. The same general behavior is seen in experimental data shown in Fig. 4(b). The amplitude of the experimental data drops off more rapidly than predicted, but the peak frequency shift is almost identical. While the amplitude drop shows some discrepancy, it is significant that even with the approximations used in the model the qualitative behavior is quite good.

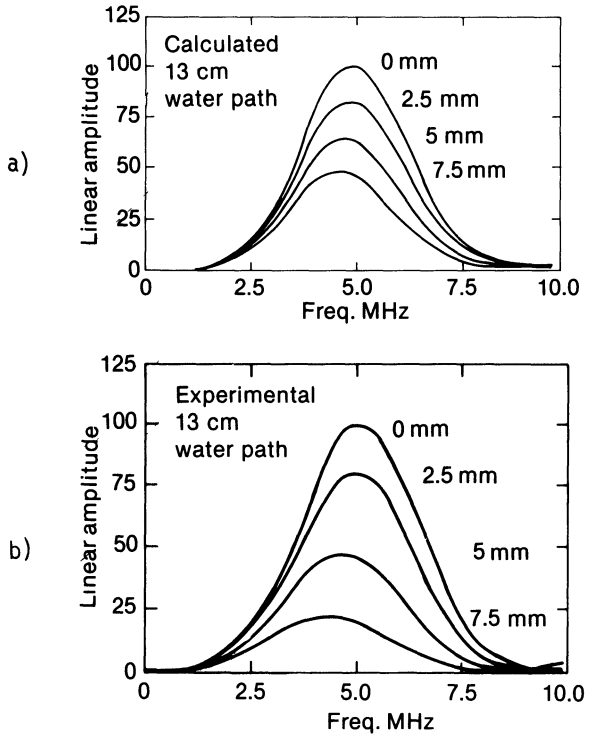

Fig. 4. Calculated (a) and measured (b) spectra from a 6-mm EDM notch at four transducer positions. Maximum amplitude is at 0 mm.

A second comparison for four different size flaws using the same transducer and geometry as in Fig. 4(a) is shown in Figs. 5(a) and 5(b). In this case the peak frequency shifts to higher frequencies as the flaw size is decreased. This is consistent with smaller flaws sampling the center portion of the field where the higher frequency components are concentrated. Agreement with experiment is again quite good and shows that the model is at least approximating the physics of the interaction.

An interesting comparison is obtained when one attempts to model the interaction as the flaw size increases to relatively large dimensions with respect to the refracted sound field. Figs. 6(a) and 6(b) show such a comparison for a 2.25 MHz, 12.7 mm diameter transducer at a 60-mm water path. The two targets or flaws are a 6-mm EDM notch in the stainless steel bar and the machined corner of the bar which essentially mimics a through-wall flaw. (The interest in this type of situation is sparked by the inability in some field inspections to accurately size large through-wall cracks in components.) When the sizes are input to the model code, the predicted spectra in Fig. 6(a) show the amplitude of the corner reflection to be smaller than that of the 6-mm EDM notch. This same behavior is shown in the experimental data in Fig. 6(b). This effect is more than just a transducer beam width effect since the flaw projection to

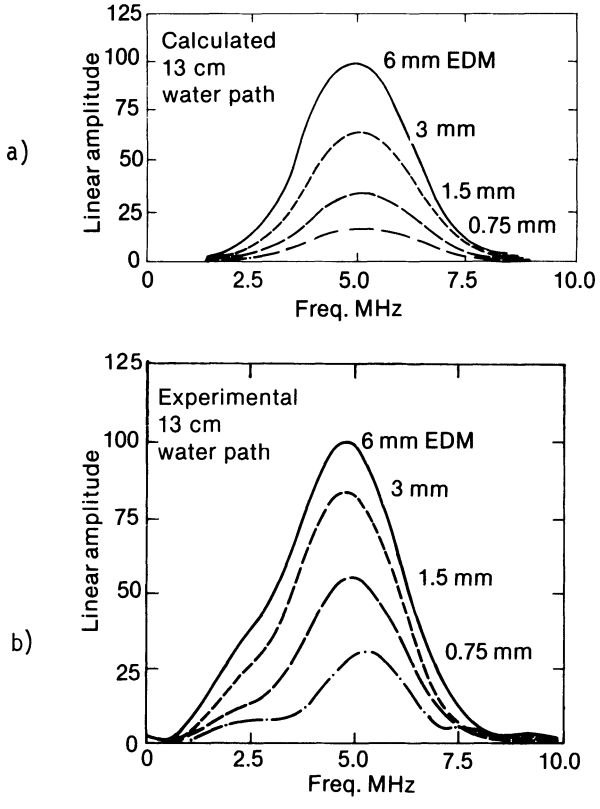

Fig. 5. Calculated (a) and measured (b) spectra from four EDM notches of different sizes. All are the maximum amplitude reflection.

the refracted shear wave is only 8.5 mm. While one expects the amplitude of the response to level off at some flaw size, it is somewhat unusual to see a decrease in amplitude. The reasons for this observed effect are still being investigated, but it is reasonable to assume that the model at least accurately predicts the leveling off of the signal.

CONCLUSIONS

Perhaps the most important conclusion that can be drawn at this point is that, for the geometries considered, the echo response is at least qualitatively predicted by considering the wavefront shape, transmission coefficients, and the angular portion of the sound field subtended by the flaw. By casting the problem in these terms, several important features of the physics of the interaction can be visualized and understood. The spectral shifts observed in the data are primarily due to the subsampling of the transducer field rather than any scattering phenomena at the flaw. This is reasonable considering the relatively large size of

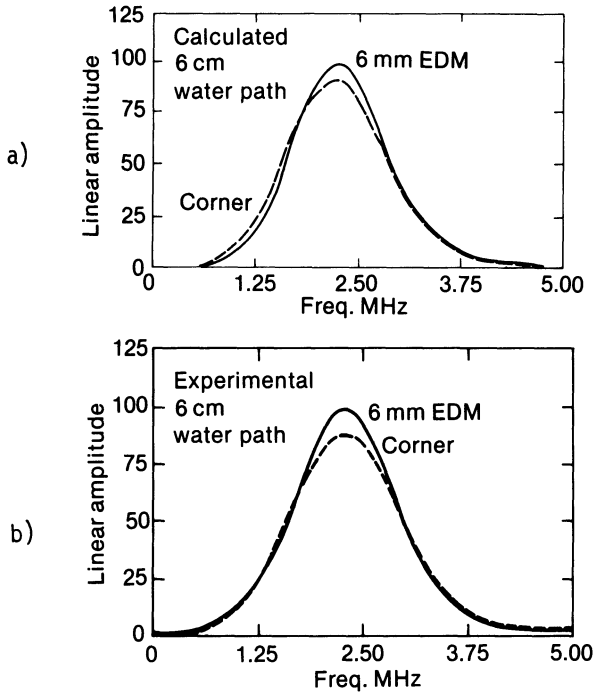

Fig. 6. Calculated (a) and measured (b) spectra from a 6-mm EDM notch and a machined corner in the same bar representing a through-wall crack.

the flaw compared to the wavelength of the ultrasound. Incorporating the wavefront shape in the model also improves the agreement between calculated and measured spectra. This is again an indication that features of the transducer field itself can be more important than the scattering from the flaw.

What is particularly useful about this formulation of the model is that it allows evaluation of the relative importance of the factors shown in Fig. 1. The model as currently implemented essentially ignores nonspecular scattering from the flaw and yet gives a good representation of the data. In a similar manner, one can exclude the transmission coefficient calculation and thus gage its overall effect on the observed signal. In this way the contribution of each aspect of the physical process can be better understood. The benefit of this is that if the model with its approximations can be made sufficiently robust, it can be used to suggest new techniques for generating and using the information contained in flaw echoes. A number of obvious improvements to the model can be incorporated.

1. The pressure distribution approximated by $2J_1(x)/x$ can be refined to more accurately represent the pressure distribution function at axial positions less than three nearfield lengths.

2. The flaw projection ray trace can be modified to more nearly approximate the complex wavefront shape variation.
3. A scattering term for flaws on the order of a wavelength can be incorporated by representing the flaw as a second radiator.
4. The calculation can be extended to three dimensions or at least the effect of comparing two dimensional calculations to three dimensional data can be evaluated.

ACKNOWLEDGMENT

This work was supported by the U.S. Department of Energy, Office of Energy Research, Office of Basic Energy Sciences under DOE Contract No. DE-AC07-ID01570.

REFERENCES

1. J. A. Johnson, "Numerical Calculations of Ultrasonic Fields: Transducer Near Fields," Journal of Nondestructive Evaluation, 3, (1), 27 (1982).
2. F. V. Ammirato, "A Calculational Model for the Shear Wave Echo from Subsurface Planar Flaws," Materials Evaluation, 34, (2), 45, (1976).
3. V. Schmitz and F. L. Becker, "Scattering of Shear Wave Pulses by Surface-Breaking Cracks - Time and Frequency Domain Analysis," Materials Evaluation, 40, (2), 191, (1982).

DISCUSSION

G.J. Gruber (Southwest Research Institute): You got me convinced fully, Basil, about the waveforms being flatter in the near field for the transducer. I had the same dilemma some years ago. I couldn't explain on the basis of spherical diverging rays why the crack tip echoes of the creeping waveform stay constant as you move the probe in and out. The only way you can explain that, if the rays go out parallel and come back parallel.

Now if I could just convince you that there are tip diffracted waves that are much better for sizing cracks than what you were doing. May I say that I believe that you are seeing tip diffracted waves in the frequency shift. As you go into larger and larger notches, you could see a shift in the frequency spectrum.

As we know, there's an inverse relationship between the time delay between the base reflected pulse and the tip diffracted pulse, and what you see in the frequency domain, the periodicity, as the cracks were getting larger or the notches were getting bigger and bigger, the tip diffracted wave was trying to come in at an earlier peak than your standard transducer frequency.

B.A. Barna: You would be absolutely right had we not gated out the tip diffracted signals so that we only analyzed the frequency content of the "root" signal from the notches. We took this approach since tip diffracted signals in real cracks can be in some cases very difficult to observe. Our approach is to develop sizing methods that rely only on the main corner reflection.

G.J. Gruber: Then I take my comment back.

B.A. Barna: But you are right, that's why we gated. It's a good point.